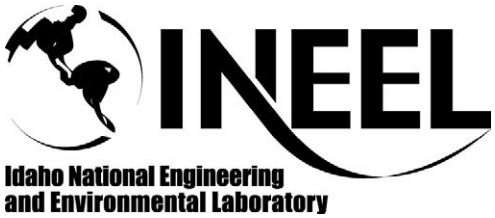

INEEL/CON-04-02301
PREPRINT

Preliminary Measurements From A New Flat Plate Facility For Aerodynamic Research

E. J. Walsh
D. Hernon
M. R. D. Davies
D. M. McEligot

March 7-11, 2005

6th European Conference On Turbo Machinery

PRELIMINARY MEASUREMENTS FROM A NEW FLAT PLATE FACILITY FOR AERODYNAMIC RESEARCH

Walsh, E.J[a*]., Hernon, D[a]., Davies, M.R.D[a]., McEligot, D.M.[b,c]

[a] Stokes Research Institute, Department of Mechanical & Aeronautical Engineering, University of Limerick, Plassey Technological Park, Limerick, Ireland, E-mail address: edmond.walsh@ul.ie , Tel. +353 61 213181[*]; Fax +353 61 202393

[b] University of Arizona, Tucson, AZ 85721,USA

[c] Idaho National Engineering and Environmental Laboratory, P.O.Box 1625, Idaho Falls, ID 83415-3885, USA

Abstract

This paper details the design and preliminary measurements used in the characterisation of a new flat plate research facility. The facility is designed specifically to aid in the understanding of entropy generation throughout the boundary layer with special attention given to non-equilibrium flows. Hot-wire measurements were obtained downstream of two turbulence generating grids. The turbulence intensity, integral and dissipation length scale ranges measured are 1.6%-7%, 5mm-17mm and 0.7mm-7mm, respectively. These values compared well to existing correlations. The flow downstream of both grids was found to be homogenous and isotropic. Flow visualisation is employed to determine aerodynamic parameters such as flow 2-dimensionality and the effect of the flap angle on preventing separation at the leading edge. The flow was found to be 2-dimensional over all measurement planes. The non-dimensional pressure distribution of a modern turbine blade suction surface is simulated on the flat plate through the use of a variable upper wall. The Reynolds number range based on wetted plate length and inlet velocity is 70,000-4,000,000.

NOMENCLATURE

C_p	Non-dimensional pressure coefficient, [-]	x	Streamwise distance, [m]
d	Grid bar width, [m]	y^+	Dimensionless wall normal distance, [-]
E(f)	1-D power spectral density, [m^2/s]	*Greek*	
f	Frequency, [Hz]	λ	Dissipation length scale, [m]
K	Thousand, [-]	Λ	Integral length scale, [m]
L_s	Suction surface length, [m]	*Subscripts*	
P	Static pressure, [N/m^2]	$(-)_d$	Grid bar width
Re	Reynolds number, [-]	$(-)_x$	x-direction
R(T)	Autocorrelation function, [-]	$(-)'$	Instantaneous
t	Time, [second]	$(-)_\infty$	Freestream
T	Time delay, [second]	$\overline{(-)}$	Time mean
Tu	x-component turbulence intensity, [-]		
u	x-component velocity, [m/s]		
U	Mean flow velocity, [m/s]		
W	Power rating, [watts]		

INTRODUCTION

Ever since the conceptual genesis of the boundary layer in the early 20th century extensive experiments have taken place to resolve its characteristics. The extent of research increased exponentially amid the realisation that the state of the boundary layer has serious implications with regard to the efficiency levels of gas turbines. Denton (1993) and Cumspty (1997) promote the understanding of entropy generation rate as the key to achieving further efficiency improvements.

For classical laminar and fully developed turbulent flows the distribution of entropy generation rate is understood and predicted reasonably well. However, knowledge is lacking for non-equilibrium flows. Such flow fields include turbulent boundary layers experiencing strong streamwise pressure gradients and flows undergoing transition from laminar to turbulent states as well as laminar boundary layers subjected to turbulent perturbations.

The most complex non-equilibrium boundary layer phenomenon is transition, which is a three dimensional, intermittent and stochastic process. This complexity is further compounded by the fact that the transition region can be significantly affected by a number of parameters. Abu-Ghannam and Shaw (1980) cite some of the factors affecting transition as being free-stream turbulence, pressure gradient, Reynolds number, Mach number, acoustic radiation, surface roughness and surface temperature. In addition, Mayle and Schulz (1996) state that the vibration of the test apparatus may also contribute to the transition process. More recently a number of authors have identified the importance of freestream turbulence properties on the transition process. Roach and Brierley (2000) suggest that it is the turbulence intensity and length scales at the leading edge that are important in determining the point of transition and not that inside the boundary layer. Jonas and Uruba (1999) established that the dissipation length scale of the oncoming flow at the leading edge had an effect on the onset and extent of transition, while Mayle (1996) derived a correlation for transition based on the length scales of turbulence. Furthermore, Choi et al (2004) found that the turbulence intensity has a major effect and the length scale has a minor effect on the pressure distributions thereby implying that turbulence intensity can cause an otherwise turbulent equilibrium boundary layer to enter a state of non-equilibrium. Thus, it is clear that any useful experimental investigation into non-equilibrium flows requires well defined boundary conditions, with particular attention paid to turbulence properties, to be truly useful for predictive code development.

Despite extensive studies over the past century on laminar, transitional and turbulent flows, few have considered the entropy generation involved. Furthermore, most of the experimental studies have lacked the measurements needed to deduce the entropy generation in the region where it is concentrated, i.e. $y^+<30$. Such an insight into the dominant loss sources and their locations allows reducing them intelligently, thereby improving efficiency.

The current research is a collaborative effort between EU and US institutes to meet the overarching scientific goal of providing new fundamental measurements and predictions of local entropy generation rates in non-equilibrium flows. This paper details a new flat plate and variable wall experimental facility at the University of Limerick using anemometry, flow visualisation and pressure measurements. The next phase of this work will be the implementation of thermal anemometry and PIV to obtain entropy generation measurements in non-equilibrium flows using the facility described herein.

EXPERIMENTAL FACILITY AND MEASURING TECHNIQUES

The wind tunnel is of the non-return type with continuous airflow supplied by a centrifugal fan. The fan is driven by a 70KW electric motor which is controlled by an electronic frequency converter. The settling chamber consists of honeycomb and wire gauze grids which enable the reduction of flow disturbances generated by the fan, as detailed by Walsh (2003). The test section dimensions are 1m in length by 0.3m width and height.

The flat plate is manufactured from 10mm thick aluminium and is approximately 1m long by 0.295m wide. A diagram of the flat plate and the test section is illustrated in figure 1. The leading edge of the plate is 2mm thick, semi-cylindrical in shape and chamfered at approximately 5 degrees to the lower surface. The plate is positioned in the mid plane of the test section. The flap was designed to be adjusted to both positive and negative angles and the trailing edge diameter is 2mm. The plate is manufactured in 4 sections allowing for a range of experimental arrangements. The plate has 60 pressure tappings for the detailed measurement of pressure distributions. The variable

wall is manufactured from 2mm sheet metal. The initial 300mm is rolled to shape and the remainder of the geometry can be adjusted to shape via adjustable jacking screws.

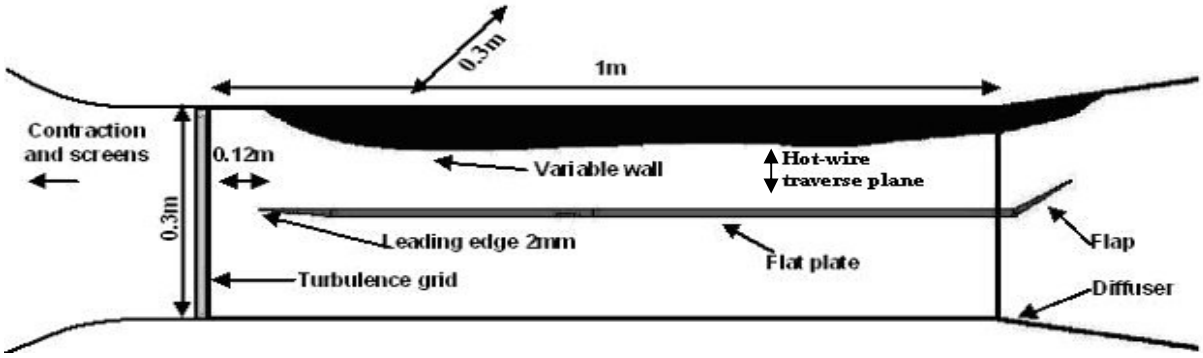

Figure 1: Diagrammatic side view of test facility (not to scale).

Gas turbine representative turbulence intensities were generated using two different turbulence generating grids. Both grids are square-hole perforated plates manufactured from 5mm thick aluminium. The grids are placed just upstream of the test section inlet. Grid 1 has a grid solidity of 42% with hole widths of 20mm and the bar width of 7mm, this corresponds to a mesh length of 34mm. The radius dimension at the corner of each hole for grid 1 is 3mm. Grid 2 has a grid solidity of 20% with hole widths of 20mm and the bar width of 2.6mm, this corresponds to a mesh length of 25.2mm. The radius dimension at the corner of each hole for grid 2 is 2mm. The bar widths for both grids were manufactured to within a tolerance of 0.1mm.

For all turbulence measurements a Dantec 56C17 constant temperature anemometer bridge was utilised to operate the hot-wire sensor in constant temperature mode, with the overheat temperature set to 250ºC. The hot-wire is of the single normal type, Dantec 55P11. The measurements were sampled at 10 KHz in 6 second blocks using a 16-bit A/D converter (DSPACE GmbH). The inlet velocity ranged from 1m/s to 60m/s for all measurements.

The pressure distributions were recorded using a digital differential pressure manometer. The freestream total pressure was obtained using a Pitot tube and the static pressures along the test surface were obtained using fifteen of the pressure tap positions. The differential pressures recorded were averaged over ten seconds.

Flow visualisation was performed on the flat plate using a mixture of powder particles and paraffin oil. The mixture used was determined through trial and error and was dependent on the velocity of the flow. The paraffin oil evaporates at standard atmospheric conditions leaving the powder particles on the test surface, thus giving a representation of the flow field, De Leeuw et al (1995). This technique allows for the visualisation of the flow 2-dimensionality and separation. In order to verify the interpretation of the oil flow visualisation results Shear Sensitive Liquid Crystals (SSLC) were used whereby a colour change response of the liquid crystal to aerodynamic shear illustrates the presence of separation regions. Further details on the use of this technique can be found in Savory et al (2000) and Reda and Wilder (2001)**.** The test surface was coated in a matt black paint to limit reflections. The SSLC should be illuminated and viewed in a direction normal to the surface on which it is applied in order to achieve the best colour response to variation in shear. In the current experimental arrangement the surface coated with the SSLC was illuminated with a white light source directly above the coating and observed from an angle of approximately 30º to the normal upstream of the test apparatus.

CHARACTERISATION OF TURBULENCE GRIDS

Roach (1987) gives an extensive review of grid types and the flow characteristics associated with them. There are generally two very important aspects of grid generated turbulence that must be taken into account during grid design. Firstly, in the initial set up region approximately 10 mesh lengths downstream of the grid the flow is highly anisotropic and inhomogeneous. Secondly, the

grid solidity must be maintained below 50 percent, otherwise flow instabilities due to jet coalescence may occur, Roach (1987) and Groth and Johansson (1988).

The decay of turbulence downstream of the grids is the first characteristic to be defined. The turbulence intensity of the flow at any point is given by equation 1.

$$Tu = \frac{\sqrt{\overline{u'^2}}}{\overline{U}} \tag{1}$$

The turbulence decay downstream of grids 1 and 2 is plotted in figure 2. It is evident from figure 2 that the turbulence intensities for grid 1 compare favourably to the Roach (1987) correlation. The difference in magnitude between the results obtained for grid 2 and the correlation is believed to be caused by the relatively high background turbulence intensity. The high background turbulence levels are currently being addressed. It is important to note, however, that the decay rate for both grids is approximately the same.

The integral length scale is calculated using equation 2 where the autocorrelation function, R(T), is given by equation 3. Non-dimensional autocorrelation functions, although not shown, compared well to the approximation given by Roach (1987).

$$\Lambda_x = U \int_0^\infty R(T)dt \tag{2}$$

$$R(T) = \frac{\overline{u'(t)u'(t-T)}}{\overline{u'^2}} \tag{3}$$

Figure 3 illustrates the comparison between the Roach (1987) correlation and the integral length scales measured using equation 2. The scatter about the correlation is comparable to that shown in Roach (1987).

To determine if the flow is isotropic, when using a single normal hot-wire probe, Roach (1987) suggests that the spectral distribution may be compared to the isotropic approximation. Such a comparison is shown in figure 4. The integral length scale may also be found using the approximation proposed by Hinze (1975), equation 4. Good agreement was found between the estimates of equation 4 and the measurements of equation 2, with a maximum deviation of 10%. Although this result is expected as the isotropic approximation is derived from the autocorrelation function, Hinze (1975), it does, however, give confidence in the analysis technique used to define the energy spectra.

$$\Lambda_x = \left[\frac{E(f)U}{4\overline{u'^2}} \right]_{f \to 0} \tag{4}$$

It is evident from figure 4 that the measured spectrum for grid 1 matches the isotropic approximation reasonably well. This agreement demonstrates that the flow is homogenous and isotropic. Corroboration that measurements should not be obtained within 10 mesh lengths downstream of the grid is also illustrated in figure 4 as the measurement taken 206mm, corresponding to 8 mesh lengths, downstream of grid 2 deviates substantially from the isotropic approximation at low frequencies. Once the turbulence is confirmed to be homogenous and isotropic the dissipation length scale can be calculated using equation 5, Roach (1987). The dissipation length scales for both grids are illustrated in figure 5 and compared to the Roach (1987) correlation, again with good agreement.

$$\left(\frac{\lambda_x}{d}\right)^2 = \frac{-10Tu}{\mathrm{Re}_d \, dTu/d(x/d)} \tag{5}$$

It is clear from the results presented that the flow characteristics downstream of both grids are well defined and match the correlations of Roach (1987) to within the level of scatter in the literature. This agreement gives confidence in both the measuring technique and the facility.

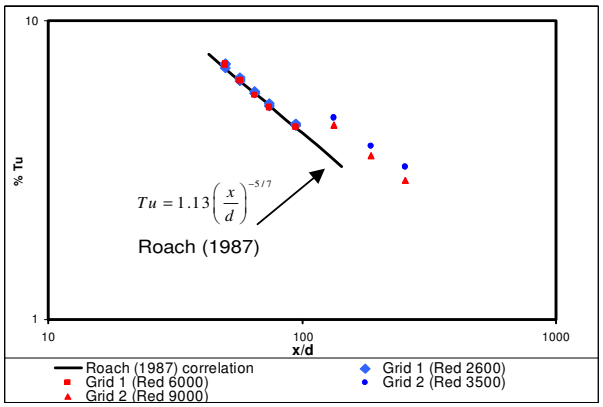

Figure 2: Turbulence intensity decay downstream of both grids.

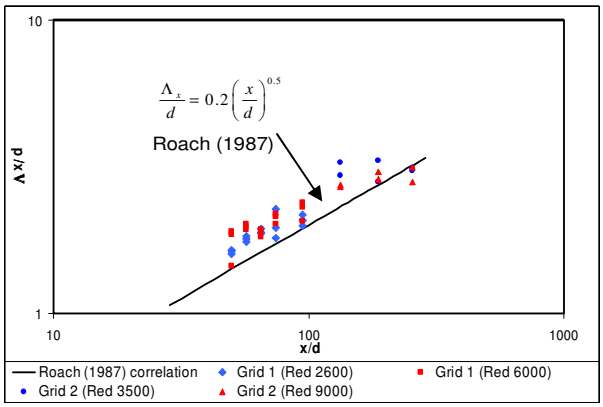

Figure 3: Integral length scale downstream of grids 1 and 2.

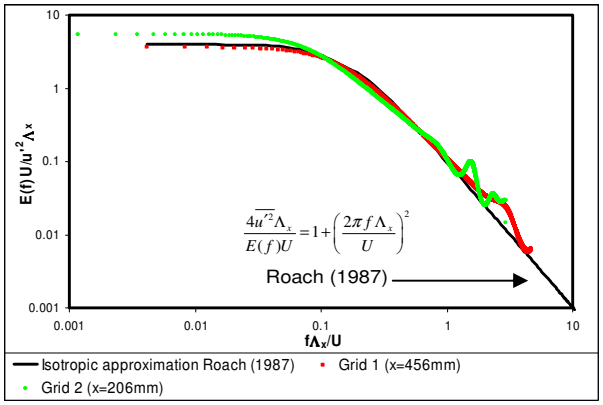

Figure 4: Spectral distributions.

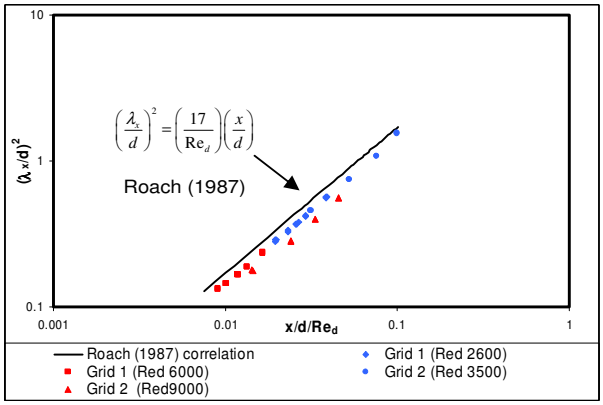

Figure 5: Dissipation length scale calculated from equation 5.

A summary of the resultant minimum and maximum values for the turbulence characteristics measured downstream of the grids are given in table 1, where minimum corresponds to approximately 10 mesh lengths downstream of the grid and maximum corresponds to the end of the test section.

Parameter	Grid 1	Grid 2
$\%Tu_{min}$	3	1.6
$\%Tu_{max}$	7	4.3
λ_{min} (mm)	1.4	0.7
λ_{max} (mm)	7	3
Λ_{min} (mm)	10	5
Λ_{max} (mm)	17	10

Table 1: Range of turbulence characteristics measured.

FLAT PLATE DESIGN, MEASUREMENTS AND FLOW VISUALISATION

Before fabrication of the test facility an investigation using a Computational Fluid Dynamics (CFD) software package, Fluent 6.1™, was undertaken in order to examine the effects of various leading and trailing edge designs on the flow field about a flat plate. Three flat plate designs were considered based on the experiments of Becker et al (2002), Jonas and Uruba (1999) and Roach and Brierley (1990).

The design of a flat plate may sound relatively simple, however, in order to match the experimental results to the existing theory a number of precautionary measures and design steps must be adhered to. There are various flat plate designs in the literature, all of which contain the same core features: (1) Elliptical or airfoil shape leading edge to prevent flow separation at the leading edge, Becker et al (2002). Thin cylindrical leading edge, approximately 2mm diameter, which is chamfered at some angle to the lower surface of the plate, Roach and Brierley (1990), Jonas and Uruba (1999) and Matsubara et al (1998). (2) Trailing edge flap and screens to adjust the circulation about the plate so as to ensure that the stagnation streamline is fixed on the upper test surface thus achieving a negligible streamwise pressure gradient, Becker et al (2002), Roach and Brierley (1990), Jonas and Uruba (1999) and Matsubara et al (1998). (3) Small gap between the plate and the side of the test section, Becker et al (2002), to hinder propagation of disturbances via the side-wall. No gap between the plate and the test section, Roach and Brierley (1990), Jonas and Uruba (1999) and Matsubara et al (1998), to ensure flow 2-dimensionality.

The three main criteria investigated in the CFD analysis of the flat plate were flow separation and shear stress distributions at the leading edge and the effectiveness of the flap design in ensuring zero pressure gradient along the plate. The distributions of shear stress at the leading edge and zero pressure gradient along the length of the plate indicated which combination of leading edge design and flap angle distorted the surrounding flow field least. From these distributions the most suitable leading edge design was found to be similar to that of Roach and Brierley (1990).

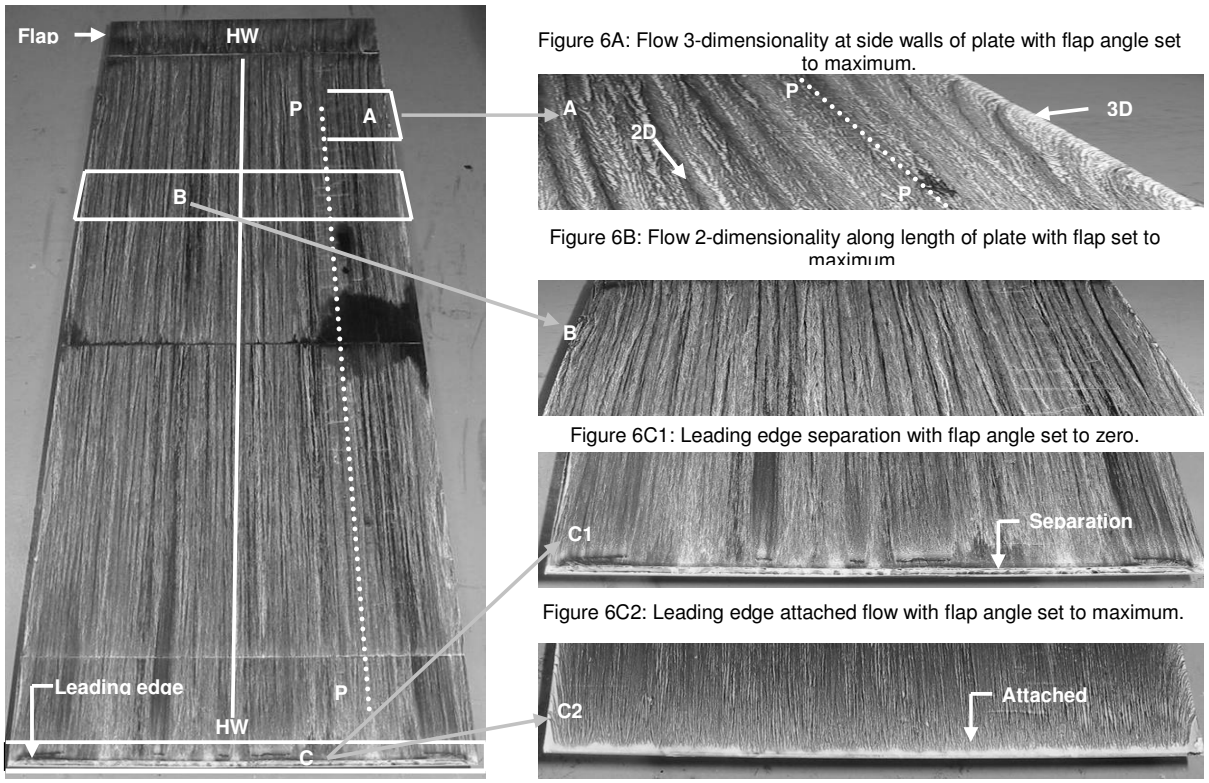

Figure 6: Flow visualisation demonstrating flow characteristics on the flat plate test surface with the flap angle set to zero and to maximum, Re_x=1.5,000,000.

In order to ensure that no adverse flow phenomena occur over the plate it is necessary to test for flow 2-dimensionality and investigate if separation develops at the leading edge. To this end, the flow visualisation technique implementing a mixture of powder particles and paraffin oil was employed, as described previously. Figure 6 illustrates the flow field on the test surface of the flat plate with the flap angle set to zero and to maximum, where maximum corresponds to approximately 40 degrees. In figure 6 the full white line denoted by HW-HW and the dotted white line denoted by P-P represent the future hot-wire traverse and pressure distribution measurement planes, respectively. When the flap angle is set to zero the flow maintains its 2-dimensionality along the length of the plate, figure 6B, and a small separation zone of the order 5mm develops at the leading edge, figure 6C1. This separation zone was also observed in CFD analysis of the flat plate. In order to prevent the development of the separation zone, thus ensuring zero streamwise pressure gradient, the flap angle is adjusted to a positive angle. The reduction in pressure on the lower surface due to the effective curvature induced by the flap causes the stagnation streamline to be firmly fixed on the upper test surface thus preventing the development of a separation zone, figure 6C2. The reorientation of the stagnation streamline was also observed in the CFD simulations using the same geometry. Although this reduction in pressure is beneficial with regard to preventing separation it has a negative affect in that it causes the flow to curve at the side walls, figure 6A. In figure 6A the area to the left of line P-P consists of 2-dimensional flow whereas to the right of this line, at the side walls of the plate, the flow is 3-dimensional. It is evident from figure 6A that, even with the flap in the most extreme position, none of the measurement planes are affected by 3-dimensional flow, this being critical for a successful experimental programme.

A SSLC mixture, Hallcrest BCN/192, was used to compliment and verify the results illustrated in figure 6. The liquid crystal has a no-shear red colour. When a shear is applied to the crystal, and the velocity vector is aligned with and directed away from the observer, a colour change response occurs. This is typically a yellow or green colour response, Reda and Wilder (2001). If the local velocity vector is directed toward the observer a non-colour change response, red/brown colour, is evident. This implies that in areas of reversed flow a red/brown colour response will be detected and at the reattachment point the SSLC will have a green/yellow colour change response. Note that in the figure 7 the raw image has been converted to a hue/saturation/lightness map in order to allow for clear demarcation in colour between the reversed and attached regions when printed in black and white.

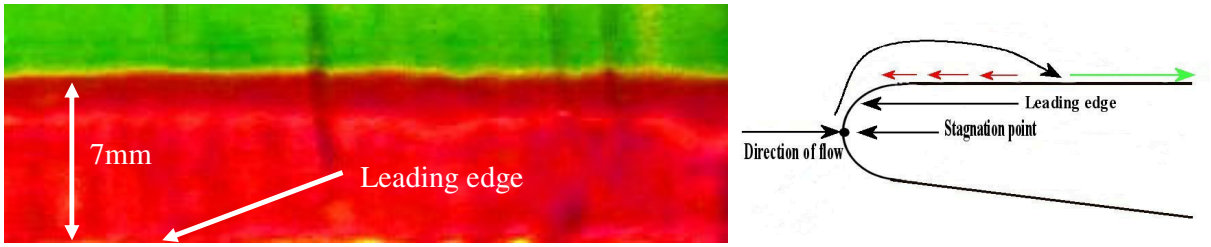

Figure 7a: Picture of SSLC at leading edge with flap in horizontal position and diagram of flow field around leading edge, Re_x=1.5,000,000.

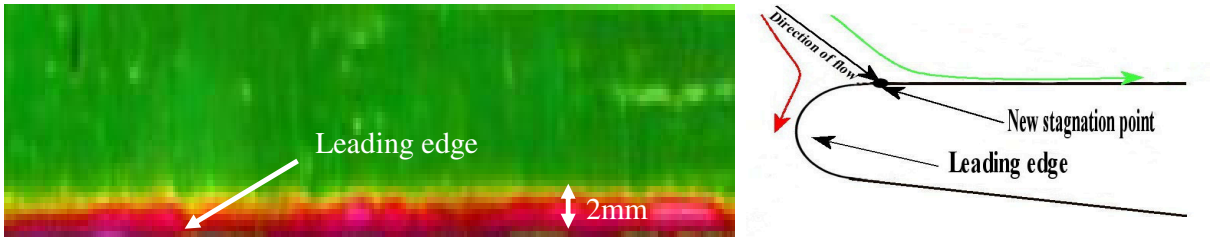

Figure 7b: Picture of SSLC at leading edge with flap in maximum position and diagram of flow field around leading edge, Re_x=1.5,000,000.

Figure 7a illustrates the SSLC visualisation of the flow at the leading edge of the plate when the flap is in the horizontal position. The liquid crystals show a reversed flow region most likely inside the separation zone of approximately 7mm in length, dark red colour, followed by attached flow marked by the green colour response. This separation zone is approximately equal in size to that observed in the oil flow visualisation for zero flap angle. Figure 7b would seem to indicate a small separation zone approximately 2mm in length, however, if one considers the dynamics of the flow around the leading edge it is clear that this is a region of reversed flow rather than a separation zone. This is due to the reorientation of the stagnation streamline as described previously. Clearly these results indicate the difficulty in comparing different facilities as different flap angles will induce scatter in data correlations.

Flat plate Pressure Distributions

The current investigation employs a flat plate on which the pressure distribution of a gas turbine blade is simulated or imposed, similar to that of Volino and Hultgren (2001), Shyne et al (2000) and Steiger (2002). There are two main advantages to this type of facility: (1) it allows for the generation of thick boundary layers to achieve high resolution measurements and (2) measurements on a flat surface are generally easier to obtain compared to the curved surface of a turbine blade.

The initial blade velocity profile to be induced over the flat plate is a high pressure turbine rotor blade designed by Santoriello et al (1993). Using a CFD analysis of the blade profile, Walsh (2003), the boundary layer edge velocity distribution was found and the variable wall shape was calculated using the continuity equation. The curved wall geometry was designed with the flap in the horizontal position as the CFD analysis demonstrated the stagnation streamline to be anchored on the upper test surface with the curved wall in place. With the curve wall in position it was found that the orientation of the flap between the horizontal and maximum position had no effect on the plate loading profile. Also, no indication of a leading edge separation zone was visualised with the flap in the horizontal position. These two effects are due to the fact that the curvature of the upper wall supersedes the effect of the flap in positioning the stagnation streamline on the upper test surface.

The non-dimensional streamwise pressure distributions are presented, figure 8, in order to demonstrate that the variable wall shape can be adjusted to approximate a given turbine blade profile. Equation 6 is the incompressible pressure coefficient, Shyne et al (2000). The design of the variable wall gives a wide range in the possible streamwise pressure distributions simulated on the plate. There is also a broad range in the Reynolds number based on the distance along the plate and inlet velocity, Re_x, with the Re_x range being approximately 70,000-4,000,000.

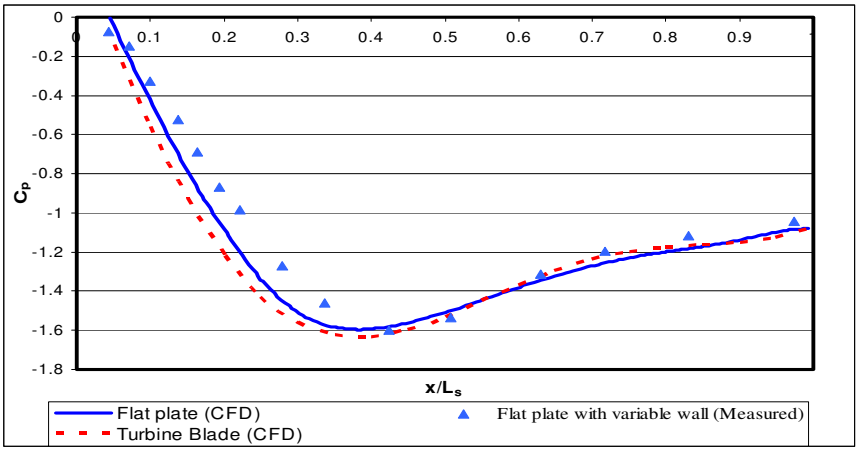

Figure 8: Non-dimensional pressure coefficient distributions using blade design of Santoriello et al (1993), Re_x=700,000.

$$C_p = (P - P_\infty) / 0.5\rho U_\infty^{\ 2} \quad (6)$$

Figure 8 illustrates the measured and predicted C_p distribution, using equation 6, over the flat plate with the variable wall in place. The comparison between both CFD results and measurements from the current facility agree favourably. This demonstrates the ability of the variable wall design to approximate a given turbine blade profile. No discontinuities in C_p were observed from measurement, thereby indicating that flow separation was suppressed in the adverse region.

CONCLUSIONS

Preliminary measurements from the new facility demonstrated that:

- Good agreement was obtained between the turbulence decay, integral and dissipation length scales downstream of both turbulence generating grids with the correlations from literature.
- By matching the spectral and length scale measurements downstream of both grids to isotropic approximations the flow was shown to be homogenous and isotropic. Using a similar method, it was also demonstrated that the flow within 10 mesh lengths of the turbulence generating grid is inhomogeneous and anisotropic.
- With the flap in the horizontal position, the flat plate flow demonstrates a high degree of 2-dimensionality along the length of the plate, although flow separation is observed at the leading edge.
- The flap is shown to modify the circulation about the plate, thus suppressing the development of a separation zone. The negative effect of this flow characteristic is the development of 3-dimensional flow in proximity to the flap at the side walls of the test section. However, the 3-dimensional effects do not interfere with the measurement regions.
- The Shear Sensitive Liquid Crystal images corroborated the interpretation of the oil and powder flow visualisation results. The images also indicated the importance of leading edge design analysis with regard to aiding in the reduction of scatter in data correlations.
- It was demonstrated that the variable wall shape can be adjusted to simulate the non-dimensional suction surface pressure profile of a modern turbine blade.

Acknowledgments

The authors wish to thank the H.T Hallowell Jr Graduate Scholarship and SFI Basic Research Grant program for financial assistance.

REFERENCES

- Abu-Ghannam, B.J., Shaw, R., (1980), "*Natural Transition of Boundary Layers-The Effects Of Turbulence, Pressure Gradient, and Flow History*", IMechE, vol. 22, No5, pp 213-228.
- Becker, S., Stoots, C.M., Condie, K.G., Durst, F., McEligot, D.M., (2002), "*LDA-Measurements of Transitional Flows Induced by a Square Rib*", J. Fluids Engineering, vol.124, pp. 108-117.
- Choi, J., Shuye, T., Han, J., Ladeinde, F., (2004), "*Effect of Free-Stream Turbulence on Turbine Blade Heat Transfer and Pressure Coefficients in Low Reynolds Number Flows*", Int. J. Heat and Mass Transfer, vol. 47, pp. 3441-3452.
- Cumpsty, N.A., (1997), "*Jet Propulsion: A Simple Guide to the Aerodynamic and Thermodynamic Design",* Cambridge University Press.
- De Leeuw, W.C., Pagendarm, H.G., Post, F.H., Walter. B., (1995), **"***Visual Simulation of Experimental Oil-Flow Visualization by Spot Noise Images from Numerical Flow Simulation"*, Proc. Eurographics Workshop in Chia, Italy , pp.135-148.
- Denton, J.D., (1993), "*Loss Mechanisms in Turbomachines",* J. Turbomachinery, vol. 115, pp. 621-654.
- Groth, J., Johansson, A.V., (1988), "*Turbulence Reduction by Screens*", J. Fluid Mech, vol. 197, pp. 139-155.

- Hinze, J.O., (1975), "*Turbulence*", McGraw-Hill Classic Textbook Reissue Series, 2nd edn.
- Jacobs, R.G., Durbin, P.A., (2001), "*Simulations of Bypass Transition",* J. Fluid Mech, vol. 428, pp. 185-212.
- Jonas, O.M., Uruba, V., (1999), "*Experiments on By-Pass Boundary Layer Transition With Several Turbulence Length Scales"*, IMechE, C557/107/99.
- Matsubara, M., Alfredsson, P.H., Westin, K.J.A., (1998), "Boundary Layer Transition at High Levels of Freestream Turbulence", ASME paper 98-GT-248.
- Mayle, R.E., Schulz, A., (1996), "The Path to Predicting Bypass Transition", ASME paper 96-GT-199.
- Reda, D.C., Wilder, M.C., (2001), "*The Shear –Sensitivity Liquid Crystal Coating Method: Visualisation of Continuous Surface Shear Stress Vector Distributions*", Von Karman Institute of Fluid Dynamics Lecture Series on Advanced Measuring Techniques.
- Roach, P.E., (1987), "*The Generation of Nearly Isotropic Turbulence by Means of Grids*", Heat and Fluid Flow, vol.8, No 2, pp. 82-92.
- Roach, P.E., Brierley, D.H., (1990), "*The Influence of a Turbulent Free-Stream on Zero Pressure Gradient Transitional Boundary Layer Development. Part 1: Test Cases T3A and T3B*.ERCOFTAC Workshop, Lausanne.
- Roach, P.E., Brierley, D.H., (2000), "*Bypass Transition Modelling: A New Method which Accounts For Free-Stream Turbulence Intensity and Length Scale*", ASME paper 2000-GT-0278.
- Santoriello, G., Colella, A., Colantuoni, S., (1993), "*Investigation of Aerodynamics and Cooling of Advanced Engine Turbine Components:-Rotor Blade Aerodynamics Design*", Brite/Euram Area 3 Aeronautics Technical Report, AER2-CT92-0044 IACA Package A.
- Savory, E., Sykes, D.M., Toy, N., (2000), "*Visualisation of Transition on an Axisymmetric Body using Shear Sensitive Liquid Crystals*", Optical Diagnogtics in Engineering, vol. 4(1), pp. 16-25.
- Shyne, R.J., Sohn, K.H., DeWitt, K.J., (2000), "*Experimental Investigation of Boundary Layer Behaviour in a Simulated Low Pressure Turbine*", J. Fluids Engineering, vol. 122, pp. 84-89.
- Steiger, R.D., (2002), "*The Effects of Wakes on Separating Boundary Layers in Low Pressure Turbines*", PhD Thesis, Cambridge University Engineering Department.
- Volino, R.J., Hultgren, L.S., (2001), "*Measurements in Separated and Transitional Boundary Layers Under Low-Pressure Turbine Airfoil Conditions",* J. Turbomachinery, vol. 123, pp. 189-197.
- Volino, R.J., Simon, T.W., (2000), "*Spectral Measurements in Transitional Boundary Layers on a Concave Wall Under High and Low Free-Stream Turbulence Conditions*", J. Turbomachinery, vol. 122, pp. 450-457.
- Wang, T., Zhou, D., (1996), "*Spectral Analysis of Boundary-Layer Transition on a Heated Flat Plate*", Int. J. Heat and Fluid Flow, vol. 17, pp. 12-21.
- Walsh, E.J., Davies, M.R.D., (2003), "*The Measurement and Prediction of Boundary Layer Entropy Generation Rate*", Paper No. IMECE2003-41380, Proceedings of IMECE'03, ASME International Mechanical Engineering Congress & Exposition Washington, D.C.